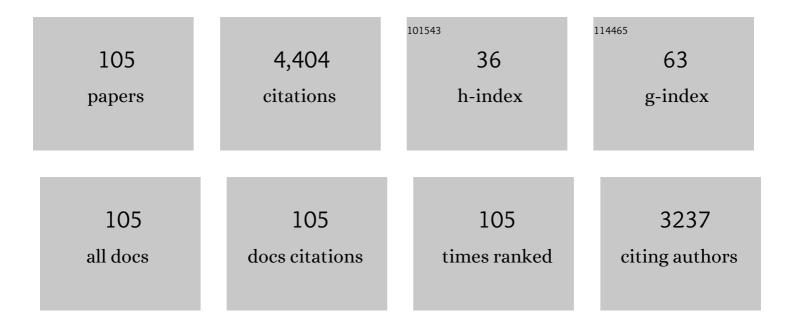
Oliver Nebel

List of Publications by Year in descending order

Source: https://exaly.com/author-pdf/4822239/publications.pdf Version: 2024-02-01



OLIVED NEREL

#	Article	IF	CITATIONS
1	Testing the advantages of simultaneous in-situ Sm Nd, U Pb and elemental analysis of igneous monazite for petrochronological studies. An example from the late Archean, Penzance granite, Western Australia. Chemical Geology, 2022, 594, 120760.	3.3	4
2	Craton Formation in Early Earth Mantle Convection Regimes. Journal of Geophysical Research: Solid Earth, 2022, 127, .	3.4	6
3	lron isotope systematics during igneous differentiation in lavas from Kīlauea and Mauna Loa, Hawai'i. Chemical Geology, 2022, 606, 120973.	3.3	2
4	Silica-rich spinel harzburgite residues formed by fractional hybridization-melting of the intra-oceanic supra-subduction zone mantle: New evidence from TUBAF seamount peridotites. Geochimica Et Cosmochimica Acta, 2021, 293, 477-506.	3.9	13
5	Heavy <mml:math <br="" xmlns:mml="http://www.w3.org/1998/Math/MathML">altimg="si46.svg"><mml:mrow><mml:mi>î</mml:mi></mml:mrow></mml:math> 57Fe in ocean island basalts: A non-unique signature of processes and source lithologies in the mantle. Geochimica Et Cosmochimica Acta. 2021, 292, 309-332.	3.9	36
6	Competing effects of spreading rate, crystal fractionation and source variability on Fe isotope systematics in mid-ocean ridge lavas. Scientific Reports, 2021, 11, 4123.	3.3	11
7	Unravelling depositional setting, age and provenance of the Simlipal volcano-sedimentary complex, Singhbhum craton: Evidence for Hadean crust and Mesoarchean marginal marine sedimentation. Precambrian Research, 2021, 354, 106038.	2.7	24
8	Formation and Evolution of a Neoproterozoic Continental Magmatic Arc. Journal of Petrology, 2021, 62, .	2.8	14
9	Molybdenum isotope systematics in cumulate rock of the 2.8 Windimurra layered intrusion: A test for igneous differentiation and the composition of the Archean mantle. Precambrian Research, 2021, 355, 106087.	2.7	7
10	Crustal rejuvenation stabilised Earth's first cratons. Nature Communications, 2021, 12, 3535.	12.8	45
11	An Early Garnet Redoxâ€Filter as an Additive Oxidizer in Lower Continental Arc Crust Traced Through Fe Isotopes. Journal of Geophysical Research: Solid Earth, 2021, 126, e2020JB021217.	3.4	2
12	Alkalinity of ocean island lavas decoupled from enriched source components: A case study from the EM1-PREMA Tasmantid mantle plume. Geochimica Et Cosmochimica Acta, 2021, 314, 140-158.	3.9	4
13	Magmatic thickening of crust in non–plate tectonic settings initiated the subaerial rise of Earth's first continents 3.3 to 3.2 billion years ago. Proceedings of the National Academy of Sciences of the United States of America, 2021, 118, .	7.1	33
14	Decoupled U-Pb date and chemical zonation of monazite in migmatites: The case for disturbance of isotopic systematics by coupled dissolution-reprecipitation. Geochimica Et Cosmochimica Acta, 2020, 269, 398-412.	3.9	35
15	Simultaneous measurement of neodymium stable and radiogenic isotopes from a single aliquot using a double spike. Journal of Analytical Atomic Spectrometry, 2020, 35, 388-402.	3.0	18
16	Magnesium isotope evidence for enhanced crustal reworking in lowermost Cambrian sedimentary rocks (Kazakhstan). Palaeogeography, Palaeoclimatology, Palaeoecology, 2020, 538, 109452.	2.3	2
17	Using apatite to resolve the age and protoliths of mid-crustal shear zones: A case study from the Taxaquara Shear Zone, SE Brazil. Lithos, 2020, 378-379, 105817.	1.4	7
18	Thermochemical lithosphere differentiation and the origin of cratonic mantle. Nature, 2020, 588, 89-94.	27.8	37

#	Article	IF	CITATIONS
19	An Early Cretaceous subduction-modified mantle underneath the ultraslow spreading Gakkel Ridge, Arctic Ocean. Science Advances, 2020, 6, .	10.3	27
20	Intraplate volcanism triggered by bursts in slab flux. Science Advances, 2020, 6, .	10.3	32
21	A coherent method for combined stable magnesium and radiogenic strontium isotope analyses in carbonates (with application to geological reference materials SARM 40, SARM 43, SRM 88A, SRM 1B). MethodsX, 2020, 7, 100847.	1.6	1
22	North Atlantic Craton architecture revealed by kimberlite-hosted crustal zircons. Earth and Planetary Science Letters, 2020, 534, 116091.	4.4	22
23	Incremental Growth of Layered Mafic-Ultramafic Intrusions Through Melt Replenishment Into a Crystal Mush Zone Traced by Fe-Hf Isotope Systematics. Frontiers in Earth Science, 2020, 8, .	1.8	7
24	Lithosphere differentiation in the early Earth controls Archean tectonics. Earth and Planetary Science Letters, 2019, 525, 115755.	4.4	38
25	Reconciling thermal regimes and tectonics of the early Earth. Geology, 2019, 47, 923-927.	4.4	44
26	A 60-Myr record of continental back-arc differentiation through cyclic melting. Nature Geoscience, 2019, 12, 215-219.	12.9	56
27	Reconciling petrological and isotopic mixing mechanisms in the Pitcairn mantle plume using stable Fe isotopes. Earth and Planetary Science Letters, 2019, 521, 60-67.	4.4	42
28	Crustal reworking at convergent margins traced by Fe isotopes in I-type intrusions from the Gangdese arc, Tibetan Plateau. Chemical Geology, 2019, 510, 47-55.	3.3	8
29	Assessment of Five Monazite Reference Materials for U-Th/Pb Dating Using Laser-Ablation ICP-MS. Geosciences (Switzerland), 2019, 9, 391.	2.2	9
30	Iron isotope exchange and fractionation between hematite (α-Fe2O3) and aqueous Fe(II): A combined three-isotope and reversal-approach to equilibrium study. Geochimica Et Cosmochimica Acta, 2019, 245, 207-221.	3.9	31
31	Radiogenic Sr and Stable C and O Isotopes Across Precambrianâ€Cambrian Transition in Marine Carbonatic Phosphorites of Malyi Karatau (Kazakhstan)—Implications for Paleoâ€environmental Change. Geochemistry, Geophysics, Geosystems, 2019, 20, 3-23.	2.5	22
32	Molybdenum isotope variations in calc-alkaline lavas from the Banda arc, Indonesia: Assessing the effect of crystal fractionation in creating isotopically heavy continental crust. Chemical Geology, 2018, 485, 1-13.	3.3	50
33	Variation in sub-arc mantle oxygen fugacity during partial melting recorded in refractory peridotite xenoliths from the West Bismarck Arc. Chemical Geology, 2018, 486, 16-30.	3.3	45
34	A non-zircon Hf isotope record in Archean black shales from the Pilbara craton confirms changing crustal dynamics ca. 3 Ga ago. Scientific Reports, 2018, 8, 922.	3.3	9
35	The Windimurra Igneous Complex: an Archean Bushveld?. Geological Society Special Publication, 2018, 453, 313-348.	1.3	11
36	Zinc isotope composition of the Earth and its behaviour during planetary accretion. Chemical Geology, 2018, 477, 73-84.	3.3	122

#	Article	IF	CITATIONS
37	Low-Ca boninite formation by second-stage melting of spinel harzburgite residues at mature subduction zones: new evidence from veined mantle xenoliths from the West Bismarck Arc. Contributions To Mineralogy and Petrology, 2018, 173, 1.	3.1	8
38	Garnet peridotites reveal spatial and temporal changes in the oxidation potential of subduction. Scientific Reports, 2018, 8, 16411.	3.3	14
39	Assessment of O and Fe isotope heterogeneity in garnet from Kakanui (New Zealand) and Erongo (Namibia). European Journal of Mineralogy, 2018, 30, 695-710.	1.3	2
40	Geological archive of the onset of plate tectonics. Philosophical Transactions Series A, Mathematical, Physical, and Engineering Sciences, 2018, 376, 20170405.	3.4	227
41	When crust comes of age: on the chemical evolution of Archaean, felsic continental crust by crustal drip tectonics. Philosophical Transactions Series A, Mathematical, Physical, and Engineering Sciences, 2018, 376, 20180103.	3.4	74
42	Iron isotope variability in ocean floor lavas and mantle sources in the Lau back-arc basin. Geochimica Et Cosmochimica Acta, 2018, 241, 150-163.	3.9	23
43	Oxidising agents in sub-arc mantle melts link slab devolatilisation and arc magmas. Nature Communications, 2018, 9, 3500.	12.8	91
44	Controls on the iron isotopic composition of global arc magmas. Earth and Planetary Science Letters, 2018, 494, 190-201.	4.4	53
45	Sulfur isotope and PGE systematics of metasomatised mantle wedge. Earth and Planetary Science Letters, 2018, 497, 181-192.	4.4	30
46	On the Sr-Nd-Pb-Hf isotope code of enriched, Dupal-type sub-continental lithospheric mantle underneath south-western China. Chemical Geology, 2018, 489, 46-60.	3.3	9
47	Strontium. Encyclopedia of Earth Sciences Series, 2018, , 1377-1379.	0.1	0
48	Rubidium. Encyclopedia of Earth Sciences Series, 2018, , 1316-1318.	0.1	0
49	Strontium Isotopes. Encyclopedia of Earth Sciences Series, 2018, , 1379-1384.	0.1	2
50	Chlorine and fluorine partition coefficients and abundances in sub-arc mantle xenoliths (Kamchatka,) Tj ETQq0 0 Geochimica Et Cosmochimica Acta, 2017, 199, 324-350.	0 rgBT /0 3.9	verlock 10 T 33
51	Silica-enriched mantle sources of subalkaline picrite-boninite-andesite island arc magmas. Geochimica Et Cosmochimica Acta, 2017, 199, 287-303.	3.9	42
52	Evidence of sub-arc mantle oxidation by sulphur and carbon. Geochemical Perspectives Letters, 2017, , 124-132.	5.0	44
53	Primary Silica-rich Picrite and High-Ca Boninite Melt Inclusions in Pyroxenite Veins from the Kamchatka Sub-arc Mantle. Journal of Petrology, 2016, 57, 1955-1982.	2.8	23
54	On the iron isotope composition of Mars and volatile depletion in the terrestrial planets. Earth and Planetary Science Letters, 2016, 449, 360-371.	4.4	39

#	Article	IF	CITATIONS
55	Iron isotope systematics in planetary reservoirs. Earth and Planetary Science Letters, 2016, 452, 295-308.	4.4	99
56	The timescales of magma evolution at mid-ocean ridges. Lithos, 2016, 240-243, 49-68.	1.4	15
57	Petrogenesis and Geochemistry of Archean Komatiites. Journal of Petrology, 2016, 57, 147-184.	2.8	96
58	The Flaw in the Crustal †Zircon Archive': Mixed Hf Isotope Signatures Record Progressive Contamination of Late-stage Liquid in Mafic†Ultramafic Layered Intrusions. Journal of Petrology, 2016, 57, 27-52.	2.8	60
59	Strontium Isotopes. Encyclopedia of Earth Sciences Series, 2016, , 1-6.	0.1	1
60	Strontium. Encyclopedia of Earth Sciences Series, 2016, , 1-3.	0.1	0
61	Rubidium. Encyclopedia of Earth Sciences Series, 2016, , 1-2.	0.1	0
62	Redox-variability and controls in subduction zones from an iron-isotope perspective. Earth and Planetary Science Letters, 2015, 432, 142-151.	4.4	74
63	Heterogeneously hydrated mantle beneath the late Archean Yilgarn Craton. Lithos, 2015, 238, 76-85.	1.4	18
64	Selective ingress of a Samoan plume component into the northern Lau backarc basin. Nature Communications, 2015, 6, 6554.	12.8	17
65	Assessment of hafnium and iron isotope compositions of Chinese national igneous rock standard materials GSR-1 (granite), GSR-2 (andesite), and GSR-3 (basalt). International Journal of Mass Spectrometry, 2015, 386, 61-66.	1.5	11
66	Combined Separation of Cu, Fe and Zn from Rock Matrices and Improved Analytical Protocols for Stable Isotope Determination. Geostandards and Geoanalytical Research, 2015, 39, 129-149.	3.1	183
67	Rb–Sr Dating. Encyclopedia of Earth Sciences Series, 2015, , 686-698.	0.1	3
68	Eoarchean within-plate basalts from southwest Greenland: REPLY. Geology, 2014, 42, e331-e331.	4.4	1
69	Refined separation of combined Fe–Hf from rock matrices for isotope analyses using AG-MP-1M and Ln-Spec chromatographic extraction resins. MethodsX, 2014, 1, 144-150.	1.6	18
70	The role of detrital zircons in Hadean crustal research. Lithos, 2014, 190-191, 313-327.	1.4	51
71	Rb–Sr Dating. , 2014, , 1-19.		8
72	Hafnium and iron isotopes in early Archean komatiites record a plume-driven convection cycle in the Hadean Earth. Earth and Planetary Science Letters, 2014, 397, 111-120.	4.4	94

#	Article	IF	CITATIONS
73	The P–T–t paths of high-grade gneisses, Kaoko Belt, Namibia: Constraints from mineral data, U–Pb allanite and monazite and Sm–Nd/Lu–Hf garnet ages and garnet ion probe data. Gondwana Research, 2014, 25, 775-796.	6.0	14
74	Maturing Arc Signatures Monitored by Trace Element and Hf Isotope Systematics in the Early Cretaceous Zacatecas Volcanic Field, Mexico. Journal of Geology, 2014, 122, 549-566.	1.4	7
75	Coupled Hf–Nd–Pb isotope co-variations of HIMU oceanic island basalts from Mangaia, Cook-Austral islands, suggest an Archean source component in the mantle transition zone. Geochimica Et Cosmochimica Acta, 2013, 112, 87-101.	3.9	40
76	Upper Zone of the Archean Windimurra layered mafic intrusion, Western Australia: insights into fractional crystallisation in a large magma chamber. Neues Jahrbuch Fur Mineralogie, Abhandlungen, 2013, 191, 83-107.	0.3	9
77	Eoarchean within-plate basalts from southwest Greenland. Geology, 2013, 41, 327-330.	4.4	27
78	Seychelles alkaline suite records the culmination of Deccan Traps continental flood volcanism. Lithos, 2013, 182-183, 33-47.	1.4	31
79	Lu–Hf isotopic memory of plume–lithosphere interaction in the source of layered mafic intrusions, Windimurra Igneous Complex, Yilgarn Craton, Australia. Earth and Planetary Science Letters, 2013, 380, 151-161.	4.4	28
80	Mo–Cr isotope evidence for a reducing Archean atmosphere in 3.46–2.76Ga black shales from the Pilbara, Western Australia. Chemical Geology, 2013, 340, 68-76.	3.3	73
81	Iron isotopic evidence for convective resurfacing of recycled arc-front mantle beneath back-arc basins. Geophysical Research Letters, 2013, 40, 5849-5853.	4.0	44
82	Hotspot trails in the South Atlantic controlled by plume and plate tectonic processes. Nature Geoscience, 2012, 5, 735-738.	12.9	78
83	Chalcophile element systematics in volcanic glasses from the northwestern Lau Basin. Geochemistry, Geophysics, Geosystems, 2012, 13, .	2.5	81
84	Origin of Meso-Proterozoic post-collisional leucogranite suites (Kaokoveld, Namibia): constraints from geochronology and Nd, Sr, Hf, and Pb isotopes. Contributions To Mineralogy and Petrology, 2012, 163, 1-17.	3.1	25
85	Coherence of the Dabie Shan UHPM Terrane Investigated by Lu–Hf and 40Ar/39Ar Dating of Eclogites. , 2011, , 325-357.		4
86	Evaluation of the 87Rb decay constant by age comparison against the U–Pb system. Earth and Planetary Science Letters, 2011, 301, 1-8.	4.4	177
87	The effect of sediment recycling in subduction zones on the Hf isotope character of new arc crust, Banda arc, Indonesia. Earth and Planetary Science Letters, 2011, 303, 240-250.	4.4	87
88	Rubidium isotopes in primitive chondrites: Constraints on Earth's volatile element depletion and lead isotope evolution. Earth and Planetary Science Letters, 2011, 305, 309-316.	4.4	46
89	Tracing the provenance and recrystallization processes of the Earth's oldest detritus at Mt. Narryer and Jack Hills, Western Australia: An in situ Sm–Nd isotopic study of monazite. Earth and Planetary Science Letters, 2011, 308, 350-358.	4.4	23
90	Precambrian sources of Early Paleozoic SE Gondwana sediments as deduced from combined Lu–Hf and U–Pb systematics of detrital zircons, Takaka and Buller terrane, South Island, New Zealand. Gondwana Research, 2011, 20, 427-442.	6.0	21

#	Article	IF	CITATIONS
91	Tungsten isotopes as tracers of core–mantle interactions: The influence of subducted sediments. Geochimica Et Cosmochimica Acta, 2010, 74, 751-762.	3.9	18
92	High-precision high field strength element partitioning between garnet, amphibole and alkaline melt from Kakanui, New Zealand. Geochimica Et Cosmochimica Acta, 2010, 74, 2741-2759.	3.9	38
93	Deep mantle storage of the Earth's missing niobium in late-stage residual melts from a magma ocean. Geochimica Et Cosmochimica Acta, 2010, 74, 4392-4404.	3.9	35
94	Reworking of Earth's first crust: Constraints from Hf isotopes in Archean zircons from Mt. Narryer, Australia. Precambrian Research, 2010, 182, 175-186.	2.7	73
95	Fluid-present melting of meta-igneous rocks and the generation of leucogranites — Constraints from garnet major- and trace element data, Lu–Hf whole rock–garnet ages and whole rock Nd–Sr–Hf–O isotope data. Lithos, 2009, 111, 220-235.	1.4	37
96	Formation and temporal evolution of the Kalahari sub-cratonic lithospheric mantle: Constraints from Venetia xenoliths, South Africa. Lithos, 2009, 112, 1069-1082.	1.4	15
97	Isotope Dilution Determinations of Lu, Hf, Zr, Ta and W, and Hf Isotope Compositions of NIST SRM 610 and 612 Glass Wafers. Geostandards and Geoanalytical Research, 2009, 33, 487-499.	3.1	51
98	An alternative model for silica enrichment in the Kaapvaal subcontinental lithospheric mantle. Geochimica Et Cosmochimica Acta, 2009, 73, 6894-6917.	3.9	21
99	Timing of thermal stabilization of the Zimbabwe Craton deduced from high-precision Rb–Sr chronology, Great Dyke. Precambrian Research, 2008, 164, 227-232.	2.7	20
100	Hafnium isotope characterization of the GJ-1 zircon reference material by solution and laser-ablation MC-ICPMS. Chemical Geology, 2008, 255, 231-235.	3.3	675
101	Hf–Nd–Pb isotope evidence from Permian arc rocks for the long-term presence of the Indian–Pacific mantle boundary in the SW Pacific. Earth and Planetary Science Letters, 2007, 254, 377-392.	4.4	70
102	Initial Hf isotope compositions in magmatic zircon from early Proterozoic rocks from the Gawler Craton, Australia: A test for zircon model ages. Chemical Geology, 2007, 241, 23-37.	3.3	106
103	Reassessment of the NBS SRM-607 K-feldspar as a high precision Rb/Sr and Sr isotope reference. Chemical Geology, 2006, 233, 337-345.	3.3	24
104	High precision determinations of 87Rb/85Rb in geologic materials by MC-ICP-MS. International Journal of Mass Spectrometry, 2005, 246, 10-18.	1.5	64
105	Spinel Harzburgite-Derived Silicate Melts Forming Sulfide-Bearing Orthopyroxenite in the Lithosphere. Part 1: Partition Coefficients and Volatile Evolution Accompanying Fluid- and Redox-Induced Sulfide Formation. Frontiers in Earth Science, 0, 10, .	1.8	3